Aeolian Research 10 (2013) 25–36

Contents lists available at SciVerse ScienceDirect

Aeolian Research

journal homepage: www.elsevier.com/locate/aeolia

Wind erosion from a sagebrush steppe burned by wildfire: Measurements of PM_{10} and total horizontal sediment flux

Natalie S. Wagenbrenner [a,c,*], Matthew J. Germino [b], Brian K. Lamb [c], Peter R. Robichaud [a], Randy B. Foltz [a]

[a] US Department of Agriculture, Forest Service, Rocky Mountain Research Station, 1221 South Main Street, Moscow, ID 83843, USA
[b] US Geological Survey, Forest and Rangeland Ecosystem Science Center, Boise, ID 83706, USA
[c] Laboratory for Atmospheric Research, Washington State University, Pullman, WA 99164, USA

ARTICLE INFO

Article history:
Available online 16 November 2012

Keywords:
Post-fire
Wind erosion
PM_{10}
Dust
Horizontal sediment flux
Vertical flux

ABSTRACT

Wind erosion and aeolian transport processes are under studied compared to rainfall-induced erosion and sediment transport on burned landscapes. Post-fire wind erosion studies have predominantly focused on near-surface sediment transport and associated impacts such as on-site soil loss and site fertility. Downwind impacts, including air quality degradation and deposition of dust or contaminants, are also likely post-fire effects; however, quantitative field measurements of post-fire dust emissions are needed for assessment of these downwind risks. A wind erosion monitoring system was installed immediately following a desert sagebrush and grass wildfire in southeastern Idaho, USA to measure wind erosion from the burned landscape. This paper presents measurements of horizontal sediment flux and PM_{10} vertical flux from the burned area. We determined threshold wind speeds and corresponding threshold friction velocities to be 6.0 and 0.20 m s^{-1}, respectively, for the 4 months immediately following the fire and 10 and 0.55 m s^{-1} for the following spring months. Several major wind erosion events were measured in the months following the July 2010 Jefferson Fire. The largest wind erosion event occurred in early September 2010 and produced 1495 kg m^{-1} of horizontal sediment transport within the first 2 m above the soil surface, had a maximum PM_{10} vertical flux of 100 mg m^{-2} s^{-1}, and generated a large dust plume that was visible in satellite imagery. The peak PM_{10} concentration measured on-site at a height of 2 m in the downwind portion of the burned area was 690 mg m^{-3}. Our results indicate that wildfire can convert a relatively stable landscape into one that is a major dust source.

Published by Elsevier B.V.

1. Introduction

Wind erosion and aeolian sediment transport processes are under studied compared to rainfall-induced soil erosion and fluvial sediment transport in post-wildfire environments. Recent work suggests that wind erosion can play a major role in burned landscapes (Ravi et al., 2007). Burned soils are susceptible to particle entrainment by wind because fire consumes protective ground cover, soil organic matter, and soil-stabilizing root networks, and can destroy naturally occurring soil crusts (Ford and Johnson, 2006), induce soil water repellency (Ravi et al., 2007), and decrease aggregate stability (Varela et al., 2010), all of which increase the wind erodibility of the soil. It will be increasingly important to understand the links between fire and post-fire wind erosion as the occurrence of wildfire is projected to increase for much of the western US in future decades due to climate change and expansion of the wildland urban interface (Flannigan et al., 2009; Theobald and Romme, 2007).

This paper presents an overview of wind erosion measured from soils burned by the 2010 Jefferson Fire on the Snake River Plain of southeastern Idaho, USA. Strong pulses of aeolian sediment transport have been reported following wildfires in this region (Sankey et al., 2009a), removing up to 5 cm of surface soil in the months following wildfire (Sankey et al., 2010) and resulting in substantial losses of soil nutrients (Hasselquist et al., 2011; Sankey et al., 2012). Fires tend to occur during the warm, dry summer period and vegetation recovery typically does not occur until the subsequent spring or summer, leaving months of bare soil exposure in which erosion varies with soil moisture and sediment supply (Sankey et al., 2009b; Sankey et al., 2012). Wind erosion does not occur or is insignificant until sites are burned in this region, and burned sites thus generate relatively high amounts of fine sediment and organic matter (Hasselquist et al., 2011) that poise newly burned sites for relatively large dust emissions. Blowing dust and ash from burned areas can impact visibility, air quality, soil productivity and nutrient transport (Sankey et al., 2012; Whicker et al., 2006), and deposition of wind-blown dust and ash can have

* Corresponding author at: US Department of Agriculture, Forest Service, Rocky Mountain Research Station, 1221 South Main Street, Moscow, ID 83843, USA. Tel.: +1 208 883 2340; fax: +1 208 883 2318.
E-mail addresses: nwagenbrenner@fs.fed.us (N.S. Wagenbrenner), germmatt@usgs.gov (M.J. Germino), blamb@wsu.edu (B.K. Lamb), probichaud@fs.fed.us (P.R. Robichaud), rfoltz@fs.fed.us (R.B. Foltz).

1875-9637/$ - see front matter Published by Elsevier B.V.
http://dx.doi.org/10.1016/j.aeolia.2012.10.003

implications for water quality (Vicars et al., 2010) and snowmelt processes (Painter et al., 2010; Rhodes et al., 2010). Additionally, contamination of croplands due to deposition of herbicide-treated soils from post-fire areas is a concern (e.g., High Country News, Issue 228, 2002).

The overall goal of this research is to quantify the role of wind erosion and corresponding impacts on air quality from the 2010 Jefferson Fire. Specific objectives were to (1) collect time-resolved measurements of horizontal sediment flux and PM_{10} vertical flux following the wildfire and (2) present these measurements in the context of surface and meteorological parameters including wind speed, friction velocity, relative humidity, soil moisture, solar radiation, air temperature, and ground cover. This study reports some of the first measurements of PM_{10} emissions from burned soils and provides a relatively comprehensive assessment of wind erosion from a post-fire environment, in terms of the modes of sediment transport monitored. We provide an overview of data collected over the 11-month monitoring period and then detail four specific wind erosion events, two in the fall following the fire and two that occurred the following spring after the snowmelt. Horizontal sediment flux is important for estimating on-site soil redistribution and associated effects, while the PM_{10} vertical flux impacts downwind air quality. The data collected during this study demonstrate the significant role that wind erosion can play in the broader environment downwind from burned sites.

2. Methods

2.1. Site description

The Jefferson Fire burned 44,110 ha of semi-arid sagebrush steppe in southeastern Idaho, USA (43°40′N, 112°35′W, elevation 1500 m) during July 2010. The fire followed a northeast trajectory and burned a strip of land nearly 50 km long and 8 km wide (Fig. 1). Wind erosion monitoring equipment was installed in the downwind (northeast) portion of the burned area roughly 2 weeks after the fire was contained. The length of the area burned upwind of the monitoring equipment was 45 km (Fig. 2).

Average precipitation at the site is 280 mm yr^{-1} and prevailing winds are from the southwest (NRCS Web Soil Survey). Soil depth ranges from 0 to greater than 200 cm and surface soils are predominantly loamy sands with up to 20% of the burned area covered by stony outcroppings of fractured basalt bedrock (NRCS Web Soil Survey). Soil surfaces directly upwind of the monitoring location were predominately loams with less than 20% rock outcroppings. Unburned soils in this ecosystem are typically protected by a naturally occurring soil crust and natural wind erosion rates are low, with an average horizontal sediment flux of 0.0003 g m^{-1} day^{-1} (Sankey et al., 2009a). The terrain is relatively flat with slopes ranging from 2% to 20%. Pre-fire vegetation was comprised primarily of Wyoming big sagebrush (*Artemisia tridentata* ssp. *wyomingenis* Rydb.) and bluebunch wheatgrass (*Agropyronspicatum* Pursh.). The fire consumed nearly all of the vegetation, leaving only the exposed root bases of the sagebrush (Fig. 3).

There was essentially no human-caused disturbance in the burned area upwind of our monitoring equipment during the study. There were a few unpaved roads located within the burn perimeter, but these were located on Idaho National Engineering Laboratory land and access was tightly restricted. There was little to no traffic on these roads during our study period. The access road we used to service the site was on BLM land about 1 km northeast (downwind) of the monitoring equipment. We accessed the site by foot from this road. The fire was contained along a county road just northeast of this access road and along Interstate-15 (both were downwind of the monitoring equipment). No fire containment lines were constructed upwind of the monitoring equipment.

2.2. Measurements

We measured horizontal sediment flux and PM_{10} concentration gradients for 11 months following fire containment in late July 2010. Horizontal sediment flux was measured at three locations along a 50-m transect normal to the prevailing wind direction using BSNE passive sediment collectors (Custom Products and Consulting, Big Spring, TX) with inlets at 5, 10, 20, 55, and 100 cm above the soil surface. The BSNE traps were located in close proximity to the PM_{10} sensors to insure that the measured PM_{10} and total horizontal sediment flux was representative of the same topography, soil conditions, and meteorological conditions. Sediment was collected from the BSNE traps roughly every 2 weeks and oven dried at 105 °C and weighed to determine sediment mass fluxes. Inlet heights were re-measured twice following substantial deflations of the soil surface elevation. PM_{10} concentration gradients were measured at two locations along the same transect as the BSNE traps using E-Sampler Particulate Sensors (MetOne Instruments, Grants Pass, OR). Real-time (5-min average) PM_{10} concentrations were monitored at 2- and 5-m heights at each location. We use the term 'peak concentration' to refer to the maximum 5-min average concentration that occurred during a particular wind event. E-Sampler PM_{10} concentrations were calibrated against concentration readings from a Beta Attenuation Monitor (E-BAM 1020, MetOne Instruments, Grants Pass, OR), which is a US EPA approved method for monitoring ambient PM_{10} concentrations (Automated Equivalent Method: EQPM-0798-122; US EPA, 2011). The calibration was performed based on laboratory wind tunnel tests in which a steady stream of burned surface soil from the study site was introduced into the tunnel and PM_{10} was measured downwind. Soil feed rates were chosen to produce PM_{10} concentrations ranging from 1 to 30 mg m^{-3} (as measured by the E-BAM). This calibration range was determined based on the capabilities of the soil feed system in our wind tunnel test chamber. Three two-min calibration tests were performed for each sampler at each concentration.

Mean winds, temperature, and turbulence were monitored with a sonic anemometer (CSAT3, Campbell Scientific, Logan, UT) operated at 10 Hz at a height of 5 m. Wind speeds were also measured with two cup-and-vane anemometers 2-m above the ground (model 014-A, Met-One, Grants Pass, OR). Hourly relative humidity, solar radiation, precipitation, soil temperature, and soil moisture were also monitored throughout the study period. Ground cover was measured monthly during the study period at six locations along two transects which began at the monitoring site and extended 100 m to the southwest. Percent ground cover was estimated for 1-m^2 plots (Fig. 4) at each location using a grid point-count method similar to methods described in Booth et al. (2005).

Vertical flux of PM_{10} (F_v) was calculated as

$$F_v = \frac{k u_* (C_1 - C_2)}{\ln\left(\frac{z_2}{z_1}\right)} \quad (1)$$

Where k is the von Karman constant, u_* is friction velocity, and C_1 and C_2 are PM_{10} concentrations at heights z_1 and z_2, respectively. This calculation assumes neutral atmospheric stability and is appropriate for the strong wind conditions that produce measureable dust fluxes. Some of the dust events measured during this study produced sufficiently large horizontal sediment fluxes to obscure the PM_{10} concentration gradient between the 2- and 5-m measurement heights. Measurement of this concentration gradient is necessary to calculate the vertical flux based on gradient transport theory, which is the basis of Eq. (1). In order to mitigate this issue and provide more reasonable estimates of PM_{10} vertical flux, we estimated PM_{10} concentrations at a height of 10 m based on a Gaussian vertical profile. The Gaussian profile is described by

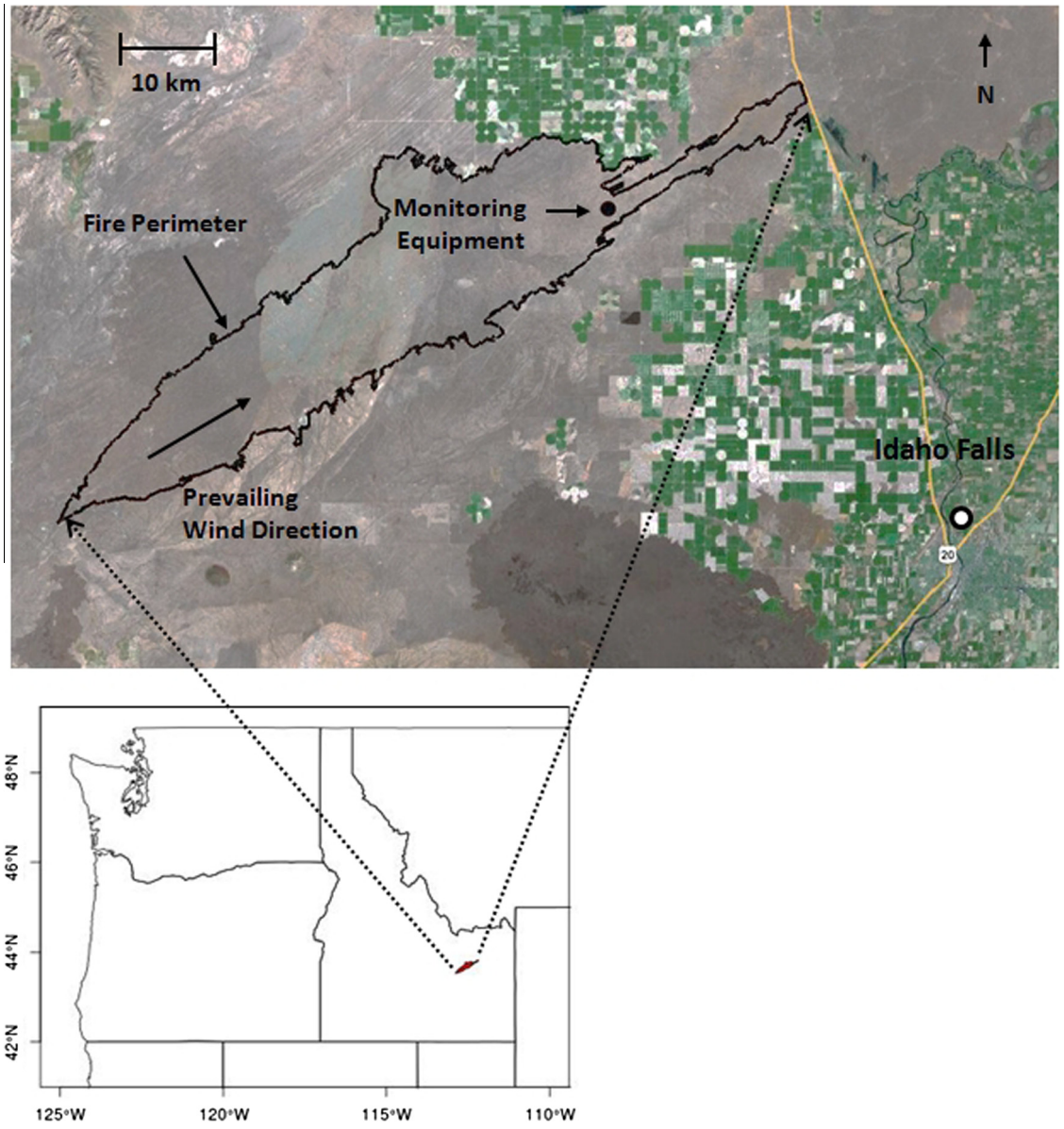

Fig. 1. Location and extent of the area burned by the Jefferson Fire. Image courtesy of Google Earth.

$$C = C_0\left(2\exp\left(-\frac{(z-h)^2}{2\sigma_z^2}\right)\right) \quad (2)$$

where C is the concentration at height z above ground, C_0 is the ground-level concentration at height $h = 0$, and σ_z is the coefficient for vertical dispersion. We estimated C_0 from Eq. (2) based on the measured concentrations at 5 m. We then used Eq. (2) with the estimated ground-level concentrations, C_0, to calculate C at a height, z, of 10 m. We assumed $\sigma_z = 3$ as a reasonable estimate of the vertical dispersion coefficient for neutral atmospheric stability (e.g., Bowne, 1974). The reported PM_{10} vertical fluxes are those calculated based on the concentration gradient between 5 m and the extrapolated concentration at 10 m. For completeness, PM_{10} vertical fluxes calculated from both methods (gradient between 2 m and 5 m and gradient between 2 m and 10 m) are reported in Fig. 6.

Horizontal sediment flux was determined for each two-week sampling interval by fitting the vertical distribution of soil mass caught by the BSNE collectors to a power function of the form

$$Q = az^{-b} \quad (3)$$

Where Q is the mass of sediment caught per unit width at each height, z, and a and b are fitted parameters. Model fits had $r^2 > 0.99$ in all cases except on 7 September 2010, when $r^2 = 0.85$, due to saturation of some collectors (four of the 15 collectors). Heights were updated to match the deflating soil surface, and the power function was integrated over 0–2 m to calculate horizontal sediment flux for each BSNE tower. Our highest BSNE inlet was 1 m above the soil surface; however, we know that sediment transport occurred above this 1-m height. Thus, we chose to integrate the derived power function to a height of 2 m in order to calculate the majority of horizontal sediment transport. The 2-m height was chosen as an appropriate cutoff because horizontal sediment flux decreases rapidly with height above the soil surface. This approach has been used in other studies (e.g., vanDonk et al., 2003). Organic matter was not removed from the BSNE-collected soils prior to analysis. There was relatively little organic material in the BSNE traps and because the density of the organic particles is much less than that of the mineral soil, the contribution of organic matter to the total mass of the sediment in the BSNE traps was negligible.

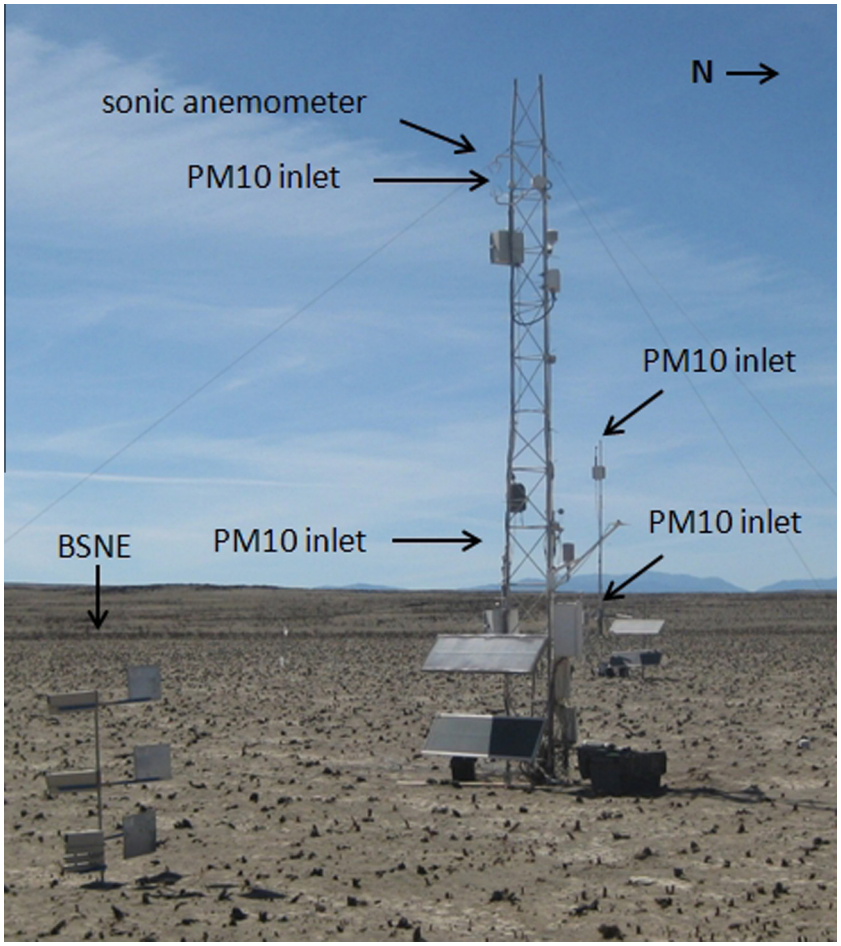

Fig. 2. Instrumentation installed at the site.

Fig. 3. Pre-fire and post-fire vegetation in the study region. Pre-fire image courtesy of the USDA Forest Service Fire and Environmental Research Applications Team (http://depts.washington.edu/nwfire/dps/).

A particle size analysis was performed on the BSNE-collected sediment with a Mastersizer particle analyzer (Malvern Instruments, Worcestershire, UK). The particle analyzer uses laser diffraction to determine the percentage of particles within discrete size bins ranging from 0.05 to 800 μm in diameter. Particle size analyses were only performed on BSNE sediment collected during three of the fall 2010 sampling periods due to equipment availability. Three replicates were performed on each BSNE bin and averaged within the bin and across the three BSNE towers to get an average particle size distribution per BSNE bin height.

We present the calculated horizontal sediment fluxes in two forms: (1) as the total flux during the sampling interval (usually about 2 weeks) and (2) as the average horizontal sediment flux on a per minute basis that is adjusted to include PM_{10} emissions were occurring. The PM_{10} data were used to determine threshold wind speeds for the fall 2010 and spring 2011 monitoring periods. We determined periods of wind erosion to be those periods when wind speeds were above the threshold wind speed for PM_{10} emissions. Presenting the flux measurements in these two forms allows the reader to (1) see the value we directly measured, total flux for

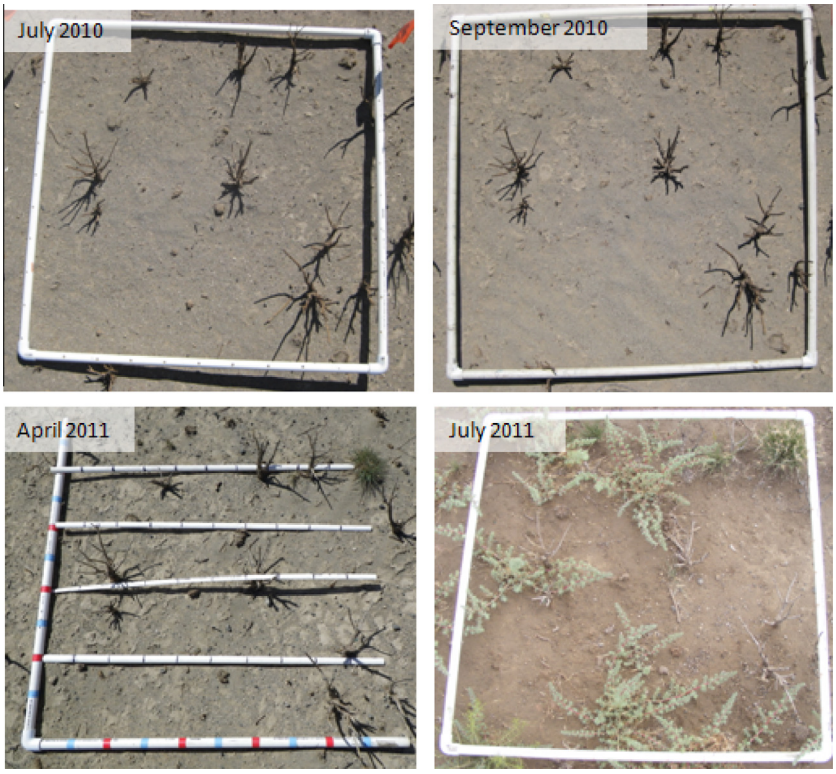

Fig. 4. Time-series photos of a single ground cover plot. Ground cover grids have dimension of 1 m × 1 m. July 2011 vegetation is *Halogeton glomerata*. Background is mineral soil.

the sampling period, and also (2) more easily compare the horizontal sediment flux to the PM_{10} vertical flux. Reporting the horizontal sediment flux averaged over only periods of wind erosion gives a better estimate of the ratio of PM_{10} vertical flux to horizontal sediment flux.

We calculated the ratio of PM_{10} vertical flux to horizontal sediment flux to provide an indication of the amount of PM_{10} emitted from the horizontal transport. There appear to be two conventions for reporting this ratio in the literature. One convention is to report the ratio with units of m^{-1}, which are the units that result from dividing PM_{10} vertical flux by horizontal sediment flux. In order to get a true ratio (i.e., dimensionless), the fetch length contributing to the BSNE measurements has to be accounted for. PM_{10} vertical flux is the flux through a plane parallel to the earth's surface. Horizontal sediment flux is the flux through a plane normal to the earth's surface. In other words, there is a footprint associated with the PM_{10} vertical flux and so the length dimension (the fetch) contributing to the horizontal sediment flux needs to be included in the calculation to account for the footprint of the BSNE measurement. We did not measure this fetch distance in our study and there does not appear to be a clear method for estimating this value in the literature. Hagen et al. (2010) reported a 250 m fetch length to reach sediment transport capacity for agricultural soils. Attempts to use this fetch distance in our study resulted in ratios that appeared to be unreasonably high (>40%) and so we report the ratio of vertical flux to horizontal transport in units of m^{-1} and without adjusting for a contributing fetch distance.

3. Results

Winds were predominantly from the southwest with maximum speeds of up to 19 m s^{-1} during this study. Winds of up to 8 m s^{-1} were also recorded from the northeast (Fig. 5). The months following the fire were relatively dry with only 82 mm of rainfall between 1 August and 3 November 2010 (Fig. 5). There was snow on the ground at the site from mid-November 2010 until late March 2011 and data were not collected during this period. The spring season was slightly wetter than the fall, with 140 mm of rainfall between 5 May and 12 July 2011 (Fig. 5). The fire consumed essentially all of the vegetation. Rock and burned roots covered 11% of the ground area immediately following the fire, leaving 89% of the area as exposed bare soil. There was no vegetation regrowth between August 2010 and March 2011. Vegetation began to reemerge in late April and by mid-June comprised 6% of the ground cover on site. Post-fire vegetation within a distance of 500 m upwind of the monitoring equipment was comprised of exotic annual halogeton (*Halogeton glomerata*) and native rabbit brush (*Chrysothamnus naseousa*). Total ground cover increased to 17% (rock, roots, and live vegetation) in July 2011 (Fig. 3).

PM_{10} vertical fluxes calculated based on concentration gradients between 2 and 5 m and 5 and 10 m are shown in Fig. 6. The vertical fluxes based on the concentration gradient between 2 and 5 m appear to be unreasonable as the vertical fluxes are larger in the spring than in the fall, although measured PM_{10} concentrations are lower in the spring than in the fall and friction velocities are comparable (Fig. 6; Fig. 7). This apparent increase in the spring vertical flux values was likely due to underestimation of the fall vertical fluxes. We suspect that the fall vertical flux values were underestimated due to the large amount of horizontal sediment transport within the surface layer which obscured the concentration gradient between the 2- and 5-m heights. Accurate measurement of the concentration gradient is necessary in order to calculate the vertical flux using Eq. (1). The calculated vertical fluxes based on the concentration gradient between 5 and 10 m appear to be more reasonable estimates and thus are the values reported in the remainder of this text.

The largest wind erosion events occurred during the 2 months following the fire (early September 2010) during periods of high

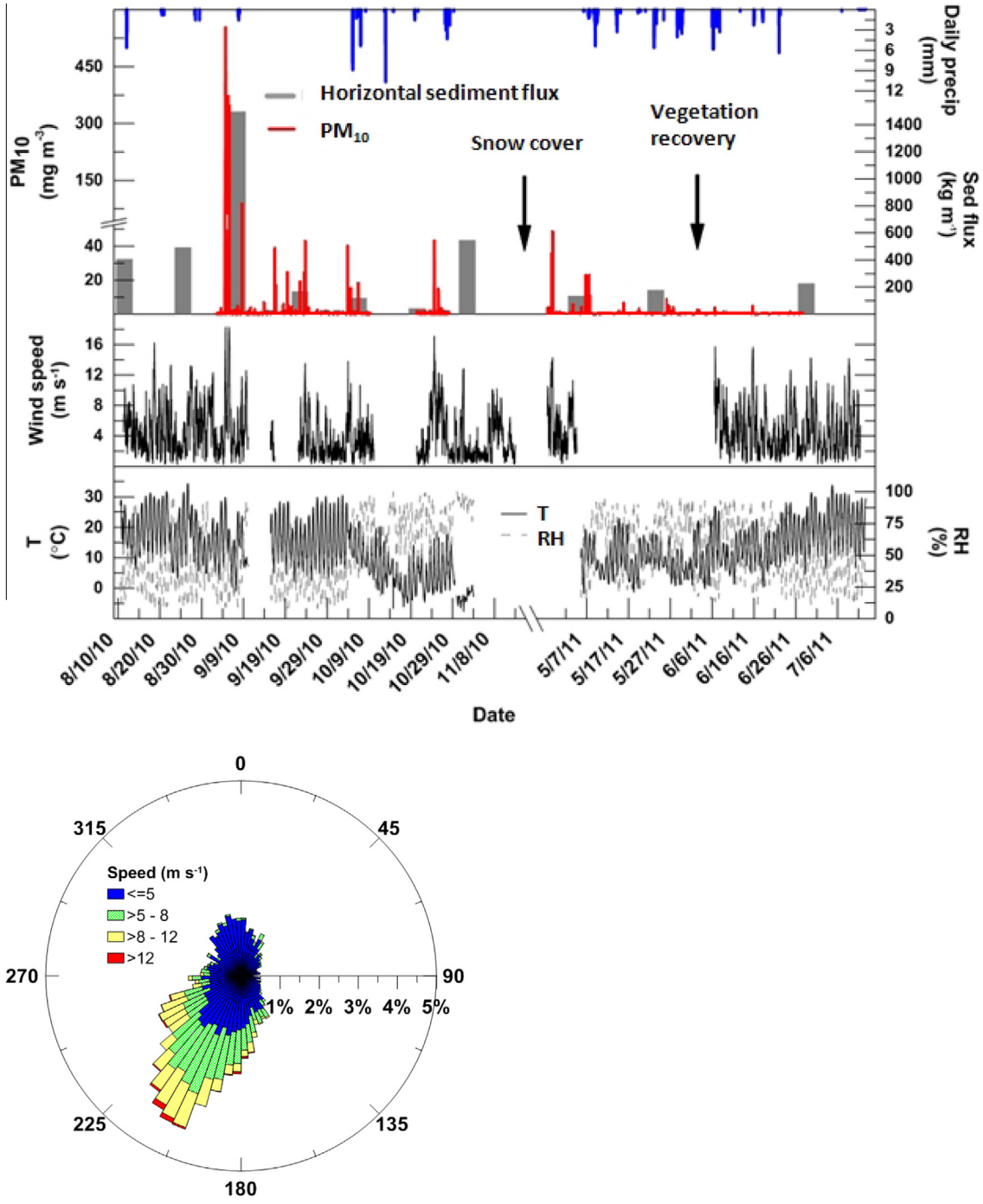

Fig. 5. Overview of post-fire meteorology and sediment transport from 10 August 2010 to 16 July 2011. PM_{10} concentrations are 5-min averages measured at 2 m above the soils surface. Horizontal sediment flux is the flux within a 2 m height above the soil surface; bars represent the total horizontal sediment flux for the sampling interval. RH is relative humidity. The length of the bars in wind rose indicates the percent of time that the wind was from a given direction.

winds and relatively dry conditions (Fig. 5). Horizontal sediment flux and PM_{10} emissions peaked during a large wind event in early September. Horizontal sediment flux and PM_{10} vertical flux decreased between mid-September and mid-October 2010 due to less frequent high-wind events and more frequent rainfall. Horizontal sediment flux increased again during a strong wind event in late October 2010 after a break in rainfall and before the snow cover arrived; we measured 0.34 kg m^{-1} min^{-1} of horizontal sediment flux during the PM_{10} emission episodes over the two-week period ending on 1 November 2010 (640 kg m^{-1} total over the 2-week period); horizontal sediment flux during this period was larger than the pre-September horizontal sediment fluxes measured in the weeks following the fire (Fig. 5). Several wind erosion events occurred following the spring snowmelt and prior to significant rainfall and vegetation re-growth. Horizontal sediment flux and PM_{10} emissions decreased from May through July 2011 as vegetation began to recover at the site.

Results from the particle size analyses showed that on average 5.3% (range of 3.2–7.5%) of the horizontal sediment flux was PM_{10} and 60% (range of 55.4–68.5) of the PM_{10} fraction was $PM_{2.5}$. The fraction of PM_{10} was relatively constant between the 29 July 2010 sample (5.9%) and the 7 September 2010 collection (6.2%), but decreased slightly during the 18 November 2010 collection (3.9%). The $PM_{2.5}$ fraction of the PM_{10} remained constant throughout the

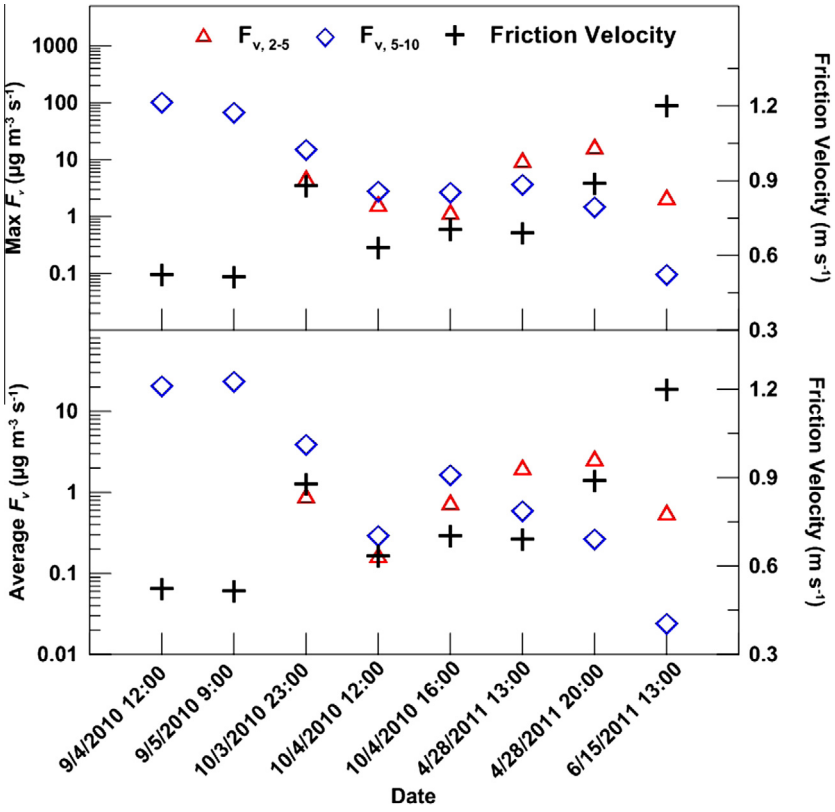

Fig. 6. Average and maximum PM_{10} vertical fluxes calculated from PM_{10} gradients above and below a height of 5 m. $F_{v,2-5}$ is the PM_{10} vertical flux calculated from the gradient between 2 and 5 m. $F_{v,5-10}$ is the PM_{10} vertical flux calculated from the gradient between 5 and 10 m. $F_{v,2-5}$ was not calculated for the 4 September or 5 September 2010 events since concentration measurements were only available at the 2-m height during these events.

fall monitoring period. Particle size analyses were not performed on the spring 2011 BSNE-collected sediment due to instrument availability.

Threshold 2-m wind speeds were determined to be 6 and 10 m s^{-1} during the fall 2010 and spring 2011 monitoring periods, respectively. Corresponding threshold friction velocities were 0.20 and 0.55 m s^{-1}. These wind speeds are frequently experienced on the Snake River Plain, which is considered to be an environment of modest to high wind energy (Jewel and Nicoll, 2011). The total number of minutes of PM_{10} emissions was determined based on the amount of time above the threshold wind speed. We estimated a total of 381 h of PM_{10} emissions over the course of 62 wind events during this field campaign. The measured peak PM_{10} concentrations during the September 2010 wind event exceeded the range of E-Sampler specifications (0–100 mg m^{-3}). The E-Sampler results did not appear to be saturated at concentrations above the certified range (i.e., the concentration readings did not plateau at an upper limit). We applied the same calibration to concentrations above this range as we did to those within the range; no additional adjustments were made. This is a limitation of the sensor and we are not aware of other PM_{10} sensors with the capability of measuring the high concentrations observed during the largest dust events at this site.

The largest calculated maximum and storm average PM_{10} vertical fluxes during this campaign were 100.0 mg m^{-2} s^{-1} and 23.2 mg m^{-2} s^{-1}, respectively. Ratios of PM_{10} vertical flux to horizontal sediment flux ranged from <0.0001 to 0.030 m^{-1}.

3.1. Specific events

The largest horizontal sediment flux and highest PM_{10} vertical flux were measured during the strongest wind event of this field campaign in early September 2010, roughly 7 weeks after the fire. The wind event occurred during the passage of a frontal system that brought sustained daytime winds of up to 19 m s^{-1} and nighttime wind speeds of 6 m s^{-1} (Fig. 7). The frequency and importance of these types of frontal systems for driving dust emissions in the Great Basin region of the western US has been previously reported (Hahnenberger and Nicoll, 2012). Early morning winds were from the northeast and stronger mid-day winds were from the southwest. The horizontal sediment flux measured during the 13-day BSNE sampling period that included this event was 1495 kg m^{-1} and 0.2 kg m^{-1} min^{-1} during the PM_{10} emission periods. Real-time PM_{10} concentrations followed trends in wind speed and friction velocity, and a peak concentration of 690 mg m^{-3} (Fig. 7) was measured on 4 September 2010 at 17:30. Calculated maximum PM_{10} vertical fluxes during the two distinct peaks shown in Fig. 6 were 100 and 68.5 mg m^{-2} s^{-1}. PM_{10} concentrations were slightly higher on 4 September than on 5 September, although observed wind speed was not notably different between the 2 days. A possible explanation that may account for the difference in PM_{10} concentrations between days was the slight shift in wind direction between days; winds were slightly more from the west on 4 September. The change in wind direction may have influenced PM_{10} concentrations at the sampling towers if the area to the west was more erodible than the area to the southwest. Another possibility is that the supply of erodible surface material was depleted during 4 September and consequently there was less material available for entrainment on 5 September.

A large dust plume originating from the burned area on 5 September 2010 was visible in MODIS satellite imagery and extended at least 100 km downwind of the source area (Fig. 8). The dust plume visible in the MODIS imagery clearly followed the mid-day southwest wind trajectory. While this trajectory did not

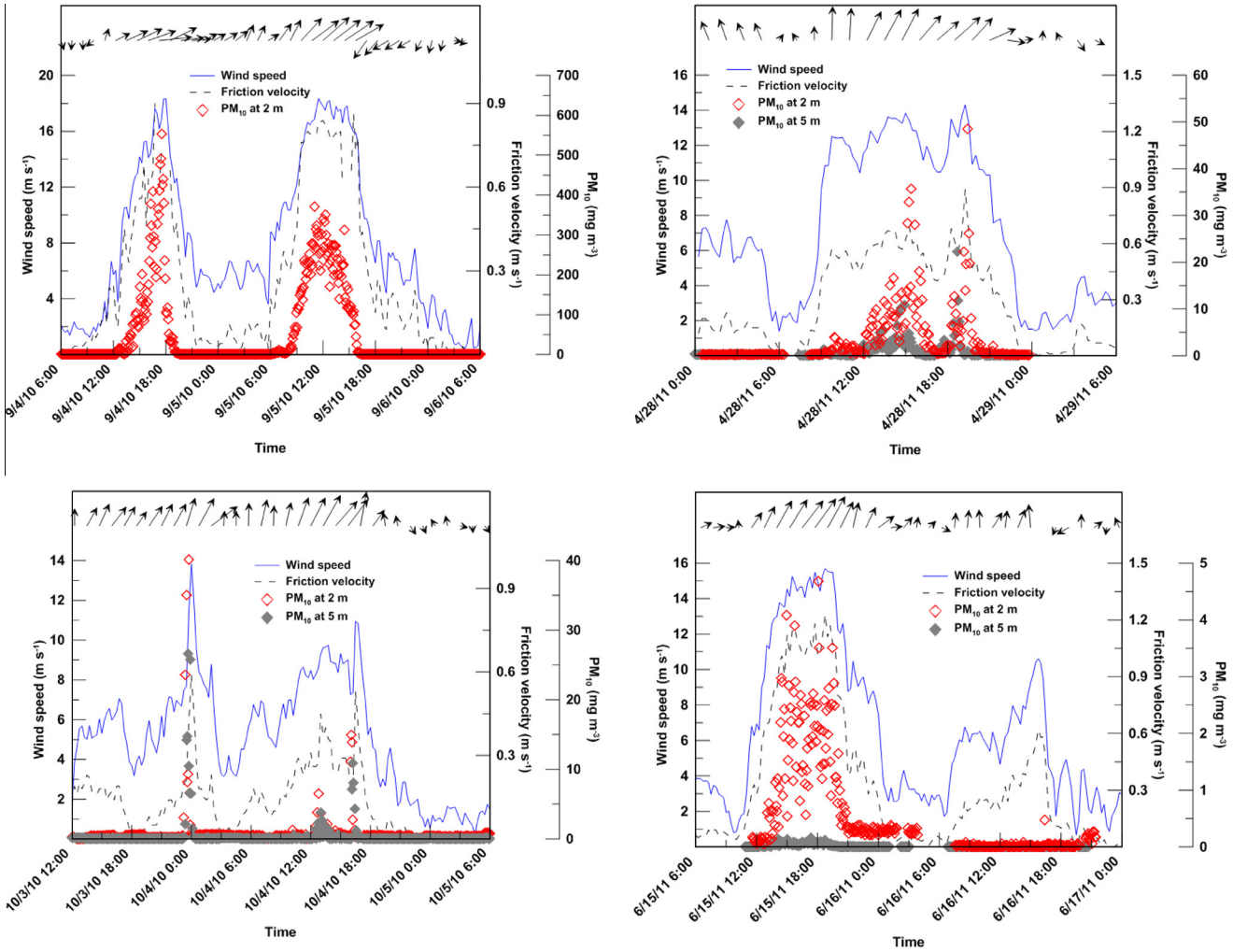

Fig. 7. Observed wind speed, wind direction, friction velocity, and PM_{10} concentrations for specific wind erosion events. PM_{10} concentrations were only measured at the 2-m height during the September 2010 event. Vectors indicate wind direction (arrow pointing to the right indicates wind from the west) and speed (magnitude of the vector). Note changes in the scale of the *y*-axis.

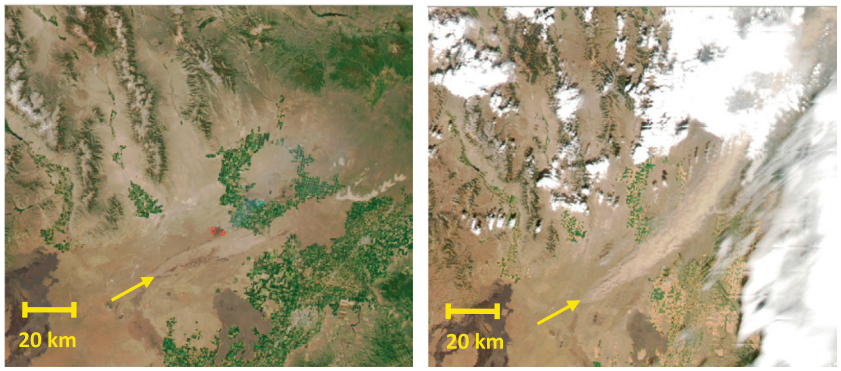

Fig. 8. MODIS Aqua satellite imagery showing the burn scar on 19 July 2010 (left) and a dust plume originating from the burned area on 5 September 2010 (right). Arrows indicate the ignition point of the fire.

impact any large population centers, it's clear from the image that this type of post-fire erosion event could have significant air quality impacts downwind of the burned area.

Another event occurred in early October 2010 when nighttime southerly winds increased to 6 m s^{-1} just before midnight on 3 October 2010 (Fig. 7). This event was smaller than the early September 2010 event and rather than producing sustained PM_{10} emissions as with the September frontal event, the October event included a series of spikes in wind speed and PM_{10} concentrations over the span of several hours. Horizontal sediment flux for the two-week period that included this event was 120.4 kg m^{-1} or 0.6 kg m^{-1} min^{-1} during the PM_{10} emission periods. The largest

Table 1
Calculated PM_{10} vertical fluxes, horizontal sediment fluxes, and ratios of PM_{10} vertical flux to horizontal sediment flux for four wind erosion events.

Event	Duration (hr)	F_v (mg m^{-2} s^{-1})		Q (kg m^{-1} min^{-1})	F_v/Q (m^{-1})	
		Max	Avg.		Max	Avg.
4–5 September 2010	28.5	100	22.0	0.20	0.0300	0.0066
3–4 October 2010	4.5	4.28	0.58	0.06	0.0150	0.0019
28 April 2011	8.0	15.9	2.21	0.09	0.0025	0.0003
15 June 2011	7.0	2.05	0.54	0.06	0.0001	<0.001

F_v is vertical flux of PM_{10}. Q is horizontal sediment flux.

spike in PM_{10} emissions occurred at midnight on 3 October when wind speed increased from around 7–14 m s^{-1} for about 10 min and PM_{10} concentrations peaked at 40.1 mg m^{-3}. Calculated maximum PM_{10} vertical fluxes during the three distinct peaks in October 2010 shown in Fig. 6 were 15.0, 2.76, and 2.63 mg m^{-2} s^{-1}. This event was notable since it occurred during nighttime conditions and had several distinct spikes in PM_{10} emissions. The spikes in PM_{10} were coincident with spikes in wind speed and demonstrate the sensitivity of the burned soils to fluctuations in wind speed.

We observed the first wind erosion event of the spring monitoring period on 28 April 2011. This event occurred during the passage of a frontal system that brought sustained southwesterly mid-day winds of 12–14 m s^{-1} (Fig. 7). The horizontal sediment flux for the 9-day BSNE sample period that included this storm was 136.8 kg m^{-1} or 0.09 kg m^{-1} min^{-1} during the PM_{10} emission periods. PM_{10} emissions began to pick up around 10:00 when wind speeds reached 12 m s^{-1}. There were two distinct peaks in PM_{10} concentrations, one around 15:00 when the wind speed reached 13 m s^{-1} and the PM_{10} concentration reached 35.7 mg m^{-3} at the 2-m height, and another larger one around 19:00 when the wind speed reached 14 m s^{-1} and the PM_{10} concentration at 2 m peaked at 50 mg m^{-3}. The maximum PM_{10} vertical fluxes during the two peaks were 3.68 and 1.49 mg m^{-2} s^{-1}.

Wind erosion tapered off by June 2011 despite frequent high-wind events. A wind event in mid-June produced a much smaller horizontal sediment flux and lower PM_{10} vertical flux than previous wind events of similar magnitude even though the 10 m s^{-1} threshold wind speed was exceeded for more than 6 h. Maximum wind speeds on 15 June were near 16 m s^{-1} and produced PM_{10} concentrations of 4.68 mg m^{-3}. Winds of up to 11 m s^{-1} on 16 June produced a maximum PM_{10} concentration of less than 1 mg m^{-3} at the 2-m height. The maximum PM_{10} vertical flux for this event was 0.095 mg m^{-2} s^{-1}. Horizontal sediment flux during this event was 0.06 kg m^{-1} min^{-1} over the PM_{10} emission period in the 36-day BSNE sampling interval.

4. Discussion

The measured horizontal sediment fluxes during the early September 2010 wind event were more than four orders of magnitude larger than values reported by Sankey et al. (2009a,b) for natural conditions in this area (Table 2). Although PM_{10} data were not available between 1 and 30 August 2010, based on observed wind speeds and horizontal sediment fluxes, we suspect that PM_{10} concentrations were elevated on a nearly daily basis, with spikes in concentration on a few particularly windy days such as 17 August (Fig. 5). Despite these suspected earlier emissions, based on the high sustained wind speeds and relative peak in horizontal sediment flux, we believe the largest PM_{10} emissions occurred during the early September 2010 event, making this event the largest in terms of both horizontal sediment flux and PM_{10} vertical flux. The MODIS satellite imagery clearly depicts the burned area as the source of dust emissions during this wind event and provides visual evidence of the areal extent of the dust emissions. The cumulative horizontal sediment flux during this episode is similar in magnitude to that reported during major wind erosion events on agricultural fields in the US (Fryrear, 1995; Table 2) and the Loess Plateau in China (Dong et al., 2010; Table 2).

Horizontal sediment fluxes and PM_{10} emissions vertical fluxes were smaller after the early September 2010 event, likely due to decreased availability of erodible surface material; however, there was substantial horizontal sediment flux in early November 2010 prior to snowfall. This indicates there was still sufficient erodible soil available to produce dust emissions. While PM_{10} emissions and horizontal sediment fluxes were smaller during mid-September 2010 to November 2010 as compared to the July 2010 to early September 2010 period, PM_{10} emissions were still in the mid to high range of values reported for agricultural soils (Fryrear, 1995; Sharratt et al., 2007; Van Pelt et al., 2004; Table 2). Peak PM_{10} concentrations measured during the September 2010 event were two orders of magnitude larger than PM_{10} concentrations reported from high wind events on the Columbia Plateau in central Washington (Sharratt et al., 2007; Table 3) and three orders of magnitude larger than those reported during high wind events on the US southern high plains (Stout, 2001; Table 3). PM_{10} vertical fluxes during fall 2010 were an order of magnitude larger than values reported for agricultural soils in the US (Sharratt et al., 2007) and on the order of the value reported by Thorsteinsson et al. (2011) for sand plains in Iceland (Table 3). PM_{10} vertical fluxes during spring 2011 were smaller than during fall 2010 but were still on the upper end of values reported for agricultural soils in the US (Sharratt et al., 2007; Sharratt and Feng, 2009; Zobeck and Van Pelt, 2006; Table 3). Ratios of PM_{10} vertical flux to horizontal sediment flux ranged from the upper end of to ten times those reported by Gillette et al. (1997) (range of 0.00005–0.05 m^{-1}) for sand, loamy sand, clay, and loam soils at a dry lake bed and up to 100 times those reported by Sharratt and Feng (2009) (range of 0.001–0.003 m^{-1}) for disturbed agricultural soils on the Columbia Plateau (Table 1).

Although smaller than the earlier September 2010 event, the October event constituted a major wind erosion episode with horizontal sediment fluxes on the same order of magnitude as those reported from large wind erosion events measured from other types of disturbed soils (Sharratt et al., 2007; vanDonk et al., 2003; Table 2) and PM_{10} vertical fluxes larger than those reported from agricultural soils (Zobeck and Van Pelt, 2006; Table 3).

The horizontal sediment flux and PM_{10} measurements made in early April 2011 were on the same order of magnitude as those measured during October 2010. Wind erosion activity in spring 2011 prompted land managers to install straw bales along a county road downwind of the fire to trap wind-blown sediment and protect the roadway (Fig. 9). By June 2011, however, vegetation began to reestablish on site and helped to stabilize the surface soils. There was a decrease in horizontal sediment flux and PM_{10} vertical flux after the vegetation started to recover. Total ground cover was still

Table 2
Horizontal sediment fluxes measured in this study compared to values reported in the literature.

Study	Location	Sediment trap[b]	Duration (days)	Horizontal sediment flux (kg m^{-1})	Measurement height (m)	Integration height[c] (m)
This study[a]	Post-fire, Snake River Plain, Idaho	BSNE	13	1495	1	2
This study[a]	Post-fire, Snake River Plain, Idaho	BSNE	14	120	1	2
Dong et al. (2010)	Loess Plateau, China	LDD	30	800	50	50
Fryrear (1995)	Elkhart, Kansas	BSNE	1	1236	2	TSS height
Fryrear (1995)	Big Spring, Texas	BSNE	1	351	2	TSS height
Fryrear (1995)	Crown Point, Indiana	BSNE	1	344	2	TSS height
Fryrear (1995)	Eads, Colorado	BSNE	1	479	2	TSS height
Fryrear (1995)	Sidney, Nebraska	BSNE	1	249	2	TSS height
Leys and McTainsh (1996)	New South Wales, Australia	BSNE	7	213	2	2.3
Nickling (1978)	Yukon, Canada	MB	<1	186	12	12
Pease et al. (2002)	Coastal Plain, North Carolina	MWAC	–	126	2.2	TSS height
Riksen and Goossens (2005)	Kootwijkerzand, Netherlands	MWAC	7	2000	1	1
Sankey et al. (2009a,b)	Post-fire, Snake River Plain, Idaho	BSNE	30	5.4	1	2
Sankey et al. (2009a,b)	Unburned, Snake River Plain, Idaho	BSNE	30	0.08	1	2
Sharratt and Feng (2009)	Columbia Plateau, Washington	BSNE	<1	1.9	1.5	5
Sharratt et al. (2007)	Columbia Plateau, Washington	BSNE	3	22	1.5	5
vanDonk et al. (2003)	Mojave Desert, California	BSNE	30	77	1	2
Van Pelt et al. (2004)	Big Spring, Texas	BSNE	1	626	1	TSS height

[a] Maximum and minimum horizontal sediment fluxes measured during this study.
[b] BSNE = Big Spring Number Eight; LDD is a modified BSNE; MB = Modified Bagnold trap; MWAC = Modified Wilson and Cooke.
[c] TSS = transition height between saltation and suspension; described in Fryrear and Saleh (1993).

Table 3
PM_{10} ambient concentrations and vertical fluxes measured in this study compared to values reported in the literature.

Study	Sensor/method	Date	Duration (hr)	Concentration (μg m^{-3})		F_v (μg m^{-2} s^{-1})		Averaging period, measurement height[a]
				Max	Avg.	Max	Avg.	
This study	E-Sampler	4 September 2010	7.5	690,000	129,000	100,000	20,820	5 min, 2 m
This study	E-Sampler	5 September 2010	11	371,000	135,000	68,520	23,180	5 min, 2 m
This study	E-Sampler	3 October 2010	1	40,200	10,100	15,000	39,10	5 min, 2 m
This study	E-Sampler	4 October 2010	2	6480	1390	2760	295	5 min, 2 m
This study	E-Sampler	4 October 2010	1.5	14,970	6390	2630	163	5 min, 2 m
This study	E-Sampler	28 April 2011	5	48,500	7310	3680	587	5 min, 2 m
This study	E-Sampler	28 April 2011	3	35,700	9030	1490	263	5 min, 2 m
This study	E-Sampler	15 June 2011	7	4680	1260	94.8	23.7	5 min, 2 m
Gillette et al. (1997)	Portable filter system	11 March 1993	1.5	–	–	–	235	–
Kjelgaard et al. (2004)	TEOM, Hi-vol	1 September 2002	13	6000	672	–	25	10 min, 3 m
Sharratt and Feng (2009)	E-Sampler, Hi-vol	29–30 August 2006	16	2580	452	–	81	5 min, 3 m
Sharratt et al. (2007)	TEOM, Hi-vol	27–29 October 2003	14	8535	791	–	255	10 min, 5 m
Thorsteinsson et al. (2011)	Back-trajectory model	2008	–	–	–	–	9720	–
Stout (2001)	Minivol	13 April 1996	24	–	166	–	–	–, 2 m
Zobeck and Van Pelt (2006)	DustTrak	18 March 2003	2.5	2000	–	400	–	1 min, 2 m

F_v is PM_{10} vertical flux.
[a] Averaging period is the period over which the time-resolved PM_{10} concentrations were averaged; this value is not reported for sensors which do not provide time-resolved PM_{10} concentrations. Measurement height is the height at which the reported concentration measurements were made.

relatively low (17%) at the end of our field campaign in July, but apparently sufficient to protect surface soils enough to attenuate sediment transport and PM_{10} vertical flux by about 33% and 93%, respectively, when the June 2011 measurements are compared to those during April 2011 (Table 1).

Vegetation recovery was facilitated by adequate spring rainfall at the site (48% of the average annual precipitation between April and July). It is possible that if the spring months had been drier than usual, the vegetation may not have recovered as quickly and dust emissions would have persisted for a longer period of time. This has been the case for other post-fire sites, such as the areas burned by the Milford Flat Complex in Utah and the Cerro Grande Fire in New Mexico, where persistent post-fire drought conditions inhibited vegetation regrowth and produced elevated dust emissions for years after the fires (Miller et al., 2012; Whicker et al., 2006) This is not an unlikely scenario as wildfires frequently occur in periods of drought that often continue into the next season and make vegetation recovery difficult and leave the soil more susceptible to erosion.

5. Conclusions

On-site horizontal sediment flux and PM_{10} concentration measurements provided a quantitative account of wind erosion in the area burned by the 2010 Jefferson Fire. We determined threshold wind speeds and corresponding threshold friction velocities to be 6.0 and 0.20 m s^{-1}, respectively for the fall 2010 period and 10 and 0.55 m s^{-1} for the spring 2011 period. Five percent of the

Fig. 9. Wind-blown sediment trapped behind straw bales protecting a county road downwind of the burned area in early April 2011, 8 months after the fire.

horizontal sediment transport was PM_{10} and 60% of the PM_{10} fraction was $PM_{2.5}$ during the 4 months following the fire. We measured a maximum PM_{10} vertical flux of 100 mg m^{-2} s^{-1} and maximum total horizontal sediment flux of 0.34 kg m^{-1} min^{-1}. To our knowledge, this is the first study to report on-site measurements of PM_{10} vertical flux from a post-fire environment in tandem with measurements of horizontal sediment flux. Horizontal sediment fluxes were sufficiently large to obscure the PM_{10} concentration gradient between 2 and 5 m above the soil surface, prohibiting calculation of PM_{10} vertical flux based on gradient transport theory within this region. To mitigate this issue, a Gaussian profile was used to estimate PM_{10} concentrations at a height of 10 m and the concentration gradient between 5 and 10 m was used to calculate PM_{10} vertical flux. This suggests that application of gradient transport theory for calculating PM_{10} vertical flux should be limited to regions above the zone of horizontal sediment transport. The extremely high PM_{10} concentrations measured in this study, in some cases, exceeded the limits of the PM_{10} sensors. The need to accurately measure on-site particle concentrations in order to quantify particle emission rates from major dust sources requires improvements to existing instrumentation or development of new measurement techniques that are more capable of handling these large particle concentrations.

These results indicate that wildfire can convert a relatively stable landscape into a highly erodible source of particulate emissions and that horizontal sediment flux and PM_{10} emissions can remain elevated for months following a fire. Burned soils can produce large horizontal sediment fluxes, comparable to those of the most wind erodible landscapes in the US, as well as high vertical fluxes of PM_{10}, with estimated values near the upper end of values reported from other types of soil disturbance.

Disclaimer

The use of trade or firm names in this report is for reader information and does not imply endorsement by the US Department of Agriculture or US Geological Survey of any product or service.

Acknowledgements

We thank Ben Kopyscianski, Robert Brown, and Cassandra Byrne from the Rocky Mountain Research Station for assistance with installation and maintenance of field equipment and Amber Hoover from Idaho State University for help with data collection and laboratory analyses. We thank Brenton Sharratt from the Agricultural Research Service for reviewing an early version of this manuscript and two anonymous reviewers whose comments improved the quality and clarity of this paper. Funding for this project was provided by the US Forest Service, US Bureau of Land Management, US Department of Defense, and the National Institute of Food and Agriculture, US Department of Agriculture, under Agreement No. 2008-38420-04761.

References

Booth, D.T., Cox, S.E., Fifield, C., Phillips, M., Williamson, N., 2005. Image analysis compared with other methods for measuring ground cover. Arid. Land. Res. Manag. 19 (2), 91–100.
Bowne, N.E., 1974. Diffusion rates. J. Air Pollut. Control Assoc. 24 (9), 832–835.
Dong, Z., Man, D., Luo, W., Qian, G., Wang, J., Zhao, M., Liu, S., Zhu, G., Zhu, S., 2010. Horizontal aeolian sediment flux in the Minqin area, a major source of Chinese dust storms. Geomorphology 116, 58–66.
Flannigan, M.D., Karwchuk, M.A., de Groot, W.J., Wotton, B.M., Gowman, L.M., 2009. Implications of changing climate for global wildland fire. Int. J. Wildland Fire 18, 483–507.
Ford, P.L., Johnson, G.V., 2006. Effects of dormant- vs. growing-season fire in short grass steppe: biological soil crust and perennial grass responses. J. Arid Environ. 67, 1–14.
Fryrear, D.W., 1995. Soil losses by wind erosion. Soil Sci. Soc. Am. J. 59, 668–672.
Fryrear, D.W., Saleh, A., 1993. Field wind erosion: vertical distribution. Soil Sci. 155, 294–300.
Gillette, D.A., Fryrear, D.W., Gill, T.E., Ley, T., Cahill, T.A., Gearhart, E.A., 1997. Relation of vertical flux of particles smaller than 10 μm to total aeolian horizontal mass flux at Owens Lake. J. Geophys. Res. 102, 26009–26015.
Hagen, L.J., van Pelt, S., Sharratt, B., 2010. Estimating the saltation and suspension components from field wind erosion. Aeolian Res. 1, 147–153.
Hahnenberger, M., Nicoll, K., 2012. Meteorological characteristics of dust storm events in the eastern Great Basin of Utah. USA. Atmos. Environ. 60, 601–612.
Hasselquist, N., Germino, M.J., Sankey, J., Glenn, N.F., Ingram, J., 2011. High potential for nutrient redistribution in aeolian sediment fluxes following wildfire in sagebrush steppe. Biogeosciences 8, 3649–3659.
High Country News, 2002. Exotic-killing herbicide is ousted from the range. Issue 228. <http://www.hcn.org/issues/228/11280> (accessed 1 March 2012).
Jewel, P.W., Nicoll, K., 2011. Wind regimes and aeolian transport in the Great Basin, USA. Geomorphology 129, 1–13.
Kjelgaard, J., Sharratt, B., Sundram, I., Lamb, B., Claiborn, C., Saxton, K., Chandler, D., 2004. PM10 emission from agricultural soils on the Columbia Plateau: comparison of dynamic and time-integrated field-scale measurements and entrainment mechanisms. Agr. Forest Meteorol. 125, 259–277.
Leys, J., McTainsh, G.H., 1996. Sediment fluxes and particulate grain-size characteristics of wind-eroded sediments in southeastern Australia. Earth Surf. Proc. Land. 21, 661–671.
Miller, M.E., Bowker, M.A., Reynolds, R.L., Goldstein, H.L., 2012. Post-fire land treatments and wind erosion – lessons from the Milford Flat Fire, UT, USA. Aeolian Res. 7, 29–44.
Nickling, W.G., 1978. Eolian sediment transport during dust storms: Slims River Valley, Yukon Territory. Can. J. Earth Sci. 15, 1069–1084.
NRCS Web Soil Survey. <http://websoilsurvey.nrcs.usda.gov/app> (accessed 1 April 2011).
Painter, T.H., Deems, J.S., Belnap, J., Hamlet, A.F., Landry, C.C., Udall, B., 2010. Response of Colorado River runoff to dust radiative forcing in snow. Proc. Natl. Acad. Sci. 107 (40), 17125–17130.
Pease, P., Gares, P., Lecce, S., 2002. Eolian dust erosion from and agricultural field on the North Carolina coastal plain. Phys. Geography 23 (5), 381–400.
Ravi, S., D'Odorico, P., Zobeck, T.M., Over, T.M., Collins, S.L., 2007. Feedbacks between fires and wind erosion in heterogeneous arid lands. J. Geophys. Res. G04007. http://dx.doi.org/10.1029/2007JG000474.
Rhodes, C., Elder, K., Greene, E., 2010. The influence of an extensive dust event on snow chemistry in the Southern Rocky Mountains. Arct. Antarct. Alpn. Res. 42 (1), 98–105.
Riksen, M.J.P.M., Goossens, D., 2005. Tillage techniques to reactivate aeolian erosion on inland drift-sand. Soil Tillage Res. 83, 218–236.
Sankey, J., Germino, M.J., Glenn, N.F., 2012. Dust supply varies with sagebrush microsites and time since burning in experimental erosion events. J. Geophys. Res. Biogeosci. http://dx.doi.org/10.1029/2011JG001724.
Sankey, J., Germino, M.J., Glenn, N., Benner, S., 2012. Transport of biologically important nutrients by wind in an eroding cold desert. Aeolian Res. 7, 17–27.
Sankey, J.B., Germino, M.J., Glenn, N.F., 2009a. Aeolian sediment transport following wildfire in sagebrush steppe. J. Arid Environ. 73, 912–919.
Sankey, J.B., Germino, M.J., Glenn, N.F., 2009b. Relationships of post-fire aeolian transport to soil and atmospheric moisture. Aeolian Res. 1, 75–85.
Sankey, J.B., Glenn, N.F., Germino, M.J., Gironella, A., Thackray, G., 2010. Relationships of aeolian erosion and deposition with LiDAR-derived landscape surface roughness following wildfire. Geomorph. 119, 135–145.
Sharratt, B.S., Feng, G., 2009. Windblown dust influenced by conventional and undercutter tillage within the Columbia Plateau, USA. Earth Surf. Proc. Land. 34, 1323–1332.

Sharratt, B., Feng, G., Wendling, L., 2007. Loss of soil and PM_{10} from agricultural fields associated with high winds on the Columbia Plateau. Earth Surf. Proc. Land. 32, 621–630.

Stout, J.E., 2001. Dust and environment in the southern high plains of North America. J. Arid Environ. 47, 425–441.

Theobald, D.M., Romme, W.H., 2007. Expansion of the US wildland–urban interface. Landscape Urban Plan. 83, 340–354.

Thorsteinsson, T., Gisladottir, G., Bullard, J., McTainsh, G., 2011. Dust storm contributions to airborne particulate matter in Reykjavik, Iceland. Atmos. Environ. 45, 5924–5933.

US EPA, Washington, D.C., 2011. 40 CFR Part 53. Ambient Air Monitoring Reference and Equivalent Methods. US EPA.

vanDonk, S.J., Huang, X., Skidmore, E.L., Anderson, A.B., Gebhart, D.L., Prehoda, V.E., Kellogg, E.M., 2003. Wind erosion from military training lands in the Mojave Desert, California, USA. J. Arid Environ. 54, 687–703.

Van Pelt, R.S., Zobeck, T.M., Potter, K.N., Stout, J.E., Popham, T.W., 2004. Validation of the wind erosion stochastic simulator (WESS) and the revised wind erosion equation (RWEQ) for single events. Eviron. Modell. Softw. 19, 191–198.

Varela, M.E., Benito, E., Keizer, J.J., 2010. Effects of wildfire and laboratory heating on soil aggregate stability of pine forests in Galicia: the role of lithology, soil organic matter content and water repellency. Catena 83, 127–134.

Vicars, W.C., Sickman, J.O., Ziemann, P.J., 2010. Atmospheric phosphorous deposition at a montane site: size distribution, effects of wildfire, and ecological implications. Atmos. Environ. 44, 2813–2821.

Whicker, J.J., Pinder, J.E., Breshears, D.D., 2006. Increased wind erosion from forest wildfire: implications for contaminant-related risks. J. Environ. Qual. 35 (2), 468–478.

Zobeck, T.M., Van Pelt, R.S., 2006. Wind-induced dust generation and transport mechanics on a bare agricultural field. J. Hazard. Mater. 132, 26–38.